

b and c physics with early ATLAS data

Nir Amram for the ATLAS Collaboration

Tel Aviv University, Tel-Aviv 69978, Israel
CERN CH-1211, Genve 23, Switzerland

DOI: will be assigned

Studies of the first $J/\psi \rightarrow \mu^+\mu^-$ and $D^{*\pm}$, D^\pm and D_s^\pm observations using the ATLAS detector, in 7 TeV proton-proton collisions at the LHC, is reported.

1 Introduction

Production of charm mesons is one of the first hard processes to be measured at the LHC. Study of the J/ψ resonance and a D^* meson signatures with early Large Hadron Collider (LHC) [1] data is one of the first goals of the ATLAS [2, 3] physics programme. Measuring the J/ψ production and properties in ATLAS is a crucial step both for understanding the detector performance and for performing measurements of various B-physics channels.

In this note we present the first studies on the J/ψ resonance of the di-muon decay channel and $D^{*\pm}$, D^\pm , D_s^\pm with the ATLAS detector using data collected in $\sqrt{s} = 7$ TeV proton-proton collisions at the LHC. The former study corresponds to an integrated luminosity of $6.4 \pm 1.3 \text{ nb}^{-1}$ and the latter to 0.37 nb^{-1} .

2 Properties of the $J/\psi \rightarrow \mu^+\mu^-$ signal

Invariant mass distributions are studied for di-muon pairs. In all cases Inner Detector (ID) [4] track parameters are used to calculate the properties of the J/ψ candidates.

An unbinned maximum-likelihood fit is used to extract the J/ψ mass and the number of J/ψ signal candidates from the data. The number of signal events N_{sig} and background events N_{bck} is calculated in the mass interval of $m_{J/\psi} \pm 3\sigma_m$.

In Figure 1 (left plot) the invariant mass for all oppositely charged muon pairs passing vertexing is shown. In the same figure, the fit function to the prompt J/ψ Monte Carlo (MC) samples, normalised to the number of signal events observed, is also shown. The fit results from data and MC are summarised in Table 1.

The invariant mass resolution depends on the pseudorapidities of the two muon tracks. In order to investigate further the measured properties of J/ψ candidates found in different regions of the detector, the candidates are divided into three categories: both muons in the barrel ($\eta < 1.05$) detector (BB); one muon in the endcap ($\eta \geq 1.05$) and one in the barrel (EB); both muons in the endcap (EE). The same mass fit is performed on each of these categories.

As expected, due to material effects, the mass width when both muons are in the endcap region is ~ 2.5 times greater than when both muons are in the barrel. This behavior is also well reproduced in the MC.

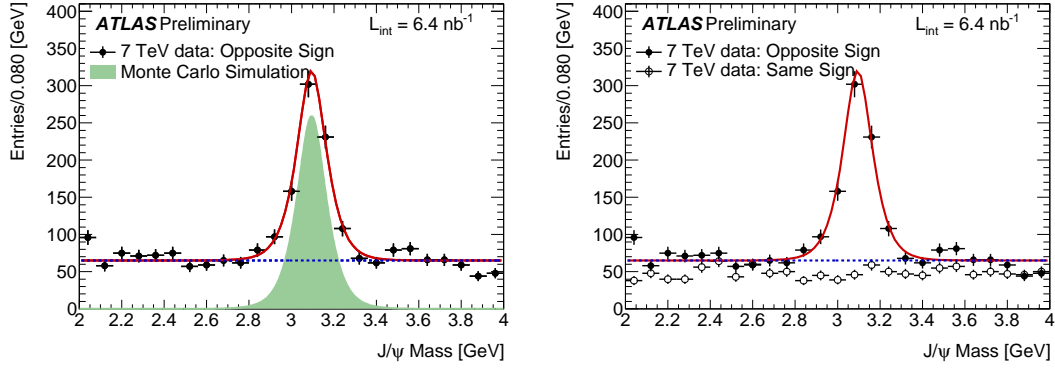


Figure 1: Invariant mass distribution of reconstructed $J/\psi \rightarrow \mu^+\mu^-$ candidates. Comparison of data to MC (left) and opposite-sign to same-sign di-muon pairs (right). The points with error bars are data. The solid line is the result of maximum likelihood unbinned fit to all di-muon pairs in the mass window 2–4 GeV and the dashed line is the result for the background of the same fit. The result of the fit to the prompt J/ψ MC is represented by solid area. Same sign combinations in open circles.

| | | $m_{J/\psi}$, GeV | σ_m , MeV | N_{sig} | N_{bck} |
|-----|------|--------------------|------------------|--------------|--------------|
| all | data | 3.095 ± 0.004 | 82 ± 7 | 612 ± 34 | 332 ± 9 |
| | MC | 3.098 ± 0.001 | 74 ± 0.4 | | |
| BB | data | 3.097 ± 0.005 | 36 ± 6 | 69 ± 9 | 8 ± 1 |
| | MC | 3.098 ± 0.001 | 37 ± 0.7 | | |
| EB | data | 3.089 ± 0.008 | 66 ± 12 | 88 ± 11 | 34 ± 3 |
| | MC | 3.097 ± 0.001 | 53 ± 0.8 | | |
| EE | data | 3.095 ± 0.006 | 88 ± 9 | 437 ± 31 | 324 ± 10 |
| | MC | 3.098 ± 0.001 | 82 ± 0.5 | | |

Table 1: Summary of fit results to mass distributions of $J/\psi \rightarrow \mu^+\mu^-$ candidates. The number of background events is given in the range $m_{J/\psi} \pm 3\sigma_m$. The same fit is applied to prompt J/ψ MC data. Results for data before vertexing are shown for comparison.

The current analysis has access to very low p_T J/ψ candidates producing soft p_T muon tracks, which are nevertheless detected in the Muon Spectrometer (MS) [5]. Muons with enough energy to cross the calorimeters reach the MS mainly in the forward region (where $p \gg p_T$). As a consequence, the J/ψ candidates in this momentum regime have preferentially high rapidity.

3 Reconstruction of Charm Mesons

$D^{*\pm}$, D^\pm and D_s^+ charm mesons were reconstructed in the range of transverse momentum $p_T(D^{(*)}) > 3.5$ GeV and pseudorapidity $|\eta(D^{(*)})| < 2.1$. Charm-meson candidates were reconstructed using tracks measured in the ATLAS inner tracking detector. We exploit the hard nature of charm fragmentation with the selections $p_T(D^*) > 3.5$ GeV, $p_T(K, \pi) > 1.0$ GeV, and $p_T(D^*)/\Sigma E_T > 0.02$, where ΣE_T is the total transverse energy in the detector.

The dE/dx particle identification was not used since it is not effective in the kinematic ranges utilized for the charm-meson reconstruction. Instead, kaon and pion masses were assumed in turn for each tracking term.

$D^{*\pm}$ mesons were identified using the decay channel $D^{*+} \rightarrow D^0 \pi_s^+ \rightarrow (K^- \pi^+) \pi_s^+$. The top left plot in Fig. 2 shows the mass difference $\Delta M = M(K\pi\pi_s) - M(K\pi)$ distribution for the $D^{*\pm}$ candidates which satisfy $1.83 < M(K\pi) < 1.90$ GeV. A clear signal is seen at the nominal value of $M(D^{*+}) - M(D^0)$. The top right plot in Fig. 2 shows the $M(K\pi)$ distribution for the $D^{*\pm}$ candidates which satisfy $144 < \Delta M < 147$ MeV. A clear signal of the D^0 mass is measured with 2100 events to be 1865.5 ± 1.4 MeV, in agreement with the PDG world average [6].

D^\pm mesons were reconstructed from the decay $D^+ \rightarrow K^- \pi^+ \pi^+$. Figure 2 shows the $M(K\pi\pi)$ distribution (bottom left) for the D^\pm candidates after all cuts. A clear signal of the D^+ mass is measured with 1667 events to be 1871.8 ± 1.1 MeV, in agreement with the PDG value. The width of the signal is in agreement with the MC expectation.

D_s^\pm mesons were reconstructed from the decay $D_s^+ \rightarrow \phi \pi^+$ with $\phi \rightarrow K^+ K^-$. The bottom right plot in Fig. 2 shows the $M(KK\pi)$ distribution for the D_s^\pm candidates with $M(KK)$ within ± 6 MeV of the nominal ϕ mass. A clear signal of the D_s^+ mass is measured with 326 events to be 1971.5 ± 4.6 MeV, in agreement with the PDG value. A smaller signal is expected around the nominal D^+ mass from the decay $D^+ \rightarrow \phi \pi^+$ with $\phi \rightarrow K^+ K^-$.

4 Summary and conclusions

The decay $J/\psi \rightarrow \mu\mu$ is observed in ATLAS data using combined information from the muon spectrometer and the inner detector. A clear peak in the data is seen with an integrated luminosity of 6.4 ± 1.3 nb $^{-1}$. The peak has been fitted using an unbinned maximum likelihood method; this yields an overall mean of 3.095 ± 0.004 GeV, which is in agreement with the PDG value for the J/ψ mass within statistical uncertainty. The signal resolution is 82 ± 7 MeV, in line with Monte Carlo expectations. The mass resolution varies with the pseudorapidity of the muons, as expected, and this variation is in agreement with Monte Carlo within statistical uncertainty. We conclude by stating that the final number of observed $J/\psi \rightarrow \mu\mu$ decays was 612 ± 34 , over a background of 332 ± 9 candidates.

Clean $D^{*\pm}$, D^\pm and D_s^\pm signals have been reconstructed with the ATLAS detector using 1.4 nb $^{-1}$ of integrated luminosity. The fitted mass values were found to be in agreement with their PDG world averages while the observed invariant mass resolution agrees with MC expectations.

B AND C PHYSICS WITH EARLY ATLAS DATA

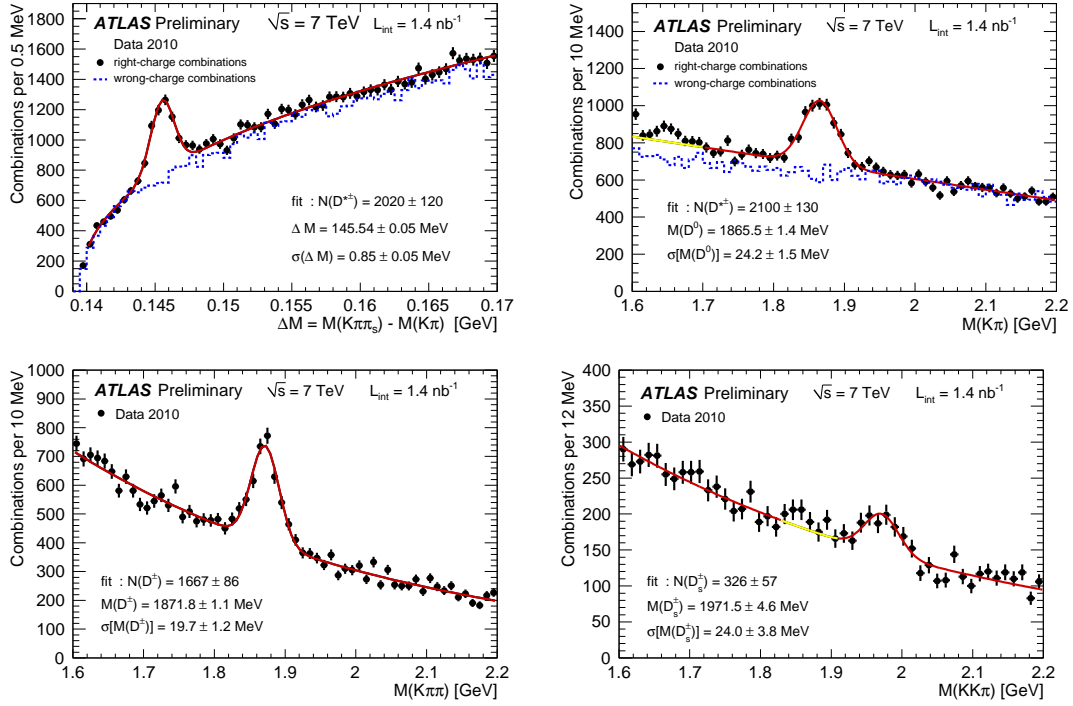


Figure 2: The distribution of the mass difference, $\Delta M = M(K\pi\pi_s) - M(K\pi)$ (top left) and the $M(K\pi)$ distribution for the $D^{*\pm}$ candidates (top right). The $M(K\pi\pi)$ distribution for the D^\pm candidates (bottom left). The $M(KK\pi)$ distribution for the D_s^\pm candidates (bottom right). The dashed histograms show the distributions for wrong-charge combinations. The solid curves represent fit results.

These studies confirm the high performance of the ATLAS detector for precision tracking measurements.

References

- [1] L. Evans and P. Bryant, *LHC machine*, JINST **3** (2008) S08001.
- [2] ATLAS Collaboration, G. Aad et al., *The ATLAS Experiment at the CERN Large Hadron Collider*, JINST **3** (2008) S08003.
- [3] C. Clement, *ATLAS first physics results*, in *Proceedings of Physics at the LHC 2010*. 2010.
- [4] ATLAS Collaboration, *ATLAS inner detector: Technical Design Report. Vol. 1*, Tech. Rep. CERN-LHCC-97-16, CERN, Geneva, Apr. 1997.
- [5] ATLAS Collaboration, *The ATLAS Muon Spectrometer Technical Design Report*, Tech. Rep. CERN-LHCC-97-22, CERN, Geneva, Mar. 1997.
- [6] PDG Collaboration, C. Amsler et al., *Review of Particle Physics*, Phys. Lett. **B667** (2008) 1.